JOURNAL OF BACTERIOLOGY, Nov. 1997, p. 7025–7032 Vol. 179, No. 22
0021-9193/97/$04.00+0

Organization and Regulation of the D-Xylose Operons in *Escherichia coli* K-12: XylR Acts as a Transcriptional Activator

SUKGIL SONG AND CHANKYU PARK*

Department of Biological Sciences, Korea Advanced Institute of Science and Technology, Yusong-Ku, Taejon, Korea

Received 23 June 1997/Accepted 3 September 1997

The metabolism of D-xylose in *Escherichia coli* K-12 is known to be mediated by the *xylAB* gene. However, the nearby *xylFGHR* genes were found by genome sequencing and predicted to be responsible for transport and regulation for xylose based on their sequence similarities to other functionally related genes. Here, we investigated transcriptional organization and functions of the *xyl* genes. An analysis with random transposon insertions revealed that the *xyl* genes are organized into two major transcriptional units, *xylAB* and *xylFGHR*, governed by the promoters P_A and P_F, respectively. However, there is an additional weak promoter, P_R, which is specific for *xylR*. Sites of transcription initiation were determined by primer extension analysis. When studied with operon fusions to *lacZ*, the P_A and P_F promoters were activated by D-xylose and repressed by glucose. In contrast, the P_R promoter was not regulated by these sugars. A mutation in *xylR* completely abolished expression from the P_A and P_F promoters, causing a defect in both growth and transport. Binding of XylR to the *xyl* promoter was enhanced by the presence of D-xylose, suggesting that transcription was positively regulated by XylR. In vivo footprinting analysis revealed that XylR binds to at least two DNA regions, I_A and I_F, each with a direct repeat. It is very likely that XylR interacts with I_A and I_F as a dimer. The presumed binding sites are located just upstream of the promoter consensus sequences (−35), while I_A is additionally flanked by a cyclic AMP receptor protein-binding site on the other side. The proposed structure of *xyl* promoters is consistent with the regulation of *xyl* gene expression and with phenotypes of transposon insertions obtained in the promoter regions.

D-Xylose is dissimilated in *Escherichia coli* K-12 through the pentose phosphate pathway (19). The sugar is first isomerized into D-xylulose by xylose isomerase (XylA) and then phosphorylated by xylulokinase (XylB) to produce D-xylulose 5-phosphate (5, 39). The transport of D-xylose with its aldopentose form is thought to be mediated by either the binding protein-dependent or the low-affinity transporter. The *xylE* gene, located at 91.4 min on the chromosome, encodes the low-affinity system that is inducible at about 10-fold by D-xylose (6). Genetic studies indicated that at least three proteins are inducible by D-xylose (5): XylA, XylB, and the transporter. In addition, genes for the xylose metabolism and the high-affinity transport were shown to be organized as an operon located at 80 min on the *E. coli* linkage map (24). A regulatory mutation affecting xylose utilization (Xyl^-) which is pleiotropic as well as recessive to the wild-type gene (34) arises at high frequency. The *xylFGH* genes involved in transport were sequenced, and their products were predicted from their similarities to *araFGH*: XylF as the xylose-binding protein, XylG as an ATP-binding protein, and XylH as a membrane transporter (43). They are linked to *xylAB* but are oriented in the opposite direction. The expression of *xylF* is negatively regulated by Fis and RpoS at the transcriptional level (50), and a putative regulator, *xylR*, was found downstream of *xylFGH*.

Study of Xyl^- mutations in *Salmonella typhimurium* LT2 indicated that there are at least four genes, *xylA*, *xylB*, *xylR*, and one for transport, that are clustered at 78 min (40). The *xylR* gene, characterized by a pleiotropic mutation, is required for the expression of other *xyl* genes. Complementation of a *xylR* mutation with F′ $xylR^+$ suggests that expression of *xylA*, *xylB*, and the transport genes is under the positive control of *xylR*. In *Staphylococcus xylosus* (42) and several *Bacillus* spp. (17, 35, 37), *xyl* genes are negatively regulated such that the repressor binds to an operator in the absence of D-xylose.

The arabinose operon, structurally similar to the *xyl* operon, receives both positive and negative modes of regulation involving AraC protein (29). The whole regulon consists of the five transcriptional units *araBAD*, *araC*, *araFGH*, *araE*, and *araJ* (4, 12, 28, 32, 47). In the *araBAD* operon, each of the two monomeric subunits of the AraC dimer interacts with either the $araO_2$ or $araI_1$ site, located far (around −200 bp) or just upstream from the P_{BAD} promoter, respectively, and thus facilitates the formation of a DNA loop in the absence of L-arabinose (7, 10, 14, 20). As a consequence, a basal level of Ara enzymes is maintained. The loop structure also suppresses *araC* transcription, which occurs in the opposite direction from that of *araBAD* (11, 14). When arabinose is present, the binding of a monomeric AraC shifts to $araI_2$ (located toward P_{BAD} as part of *araI*) from $araO_2$, thereby activating the transcription of P_{BAD} (3, 20, 29, 33). The cyclic AMP receptor protein (CRP) plays a role by binding to a region upstream of *araI*, thereby opening the loop to initiate transcription from both P_{BAD} and P_C (21). The close proximity of the CRP-binding site to the AraC-binding site suggests that interactions of the two proteins are involved in P_{BAD} activation.

In this study, transposon mutagenesis was carried out to obtain insertions and transcriptional fusions in the *xyl* genes that resulted in various degrees of growth defects on xylose. Characterizations of the insertions and the binding of XylR to the promoter region revealed that the XylR protein serves as a positive regulator by binding to two distinct regions of the *xyl* promoters. The *xylR* gene can additionally be transcribed by a weak internal promoter, P_R, that is specific for *xylR*. It is suggested that XylR binds to two distinct regions of the major *xyl* promoters as a dimer and activates transcription by closely

* Corresponding author. Phone: 82-42-869-4019. Fax: 82-42-869-2610. E-mail: ckpark@hanbit.kaist.ac.kr.

TABLE 1. *E. coli* K-12 strains and plasmids used

Strain or plasmid	Genotype and characteristics	Source or reference
Strains		
CP367	*ara his lac leu polA*(Ts) *rpsL thi thr tonA tsx xyl*	G. Hazelbauer
CP1014	F^- *araD139* Δ(*argF-lac*)*U169 deoC1 flbB530 ptsF25* Δ*rbsB4 relA1 rpsL150*	Lab collection
CP1015	CP1014 *xylA3*::Tn*phoA′*-1	This work
CP1016	CP1014 *xylA2*::Tn*phoA′*-1	This work
CP1017	CP1014 *xylA1*::Tn*phoA′*-1	This work
CP1018	CP1014 *xylG1*::Tn*phoA′*-1	This work
CP1019	CP1017 *xylG1*::Tn*phoA′*-7	This work
CP1020	CP1014 *xylR1*::Tn*phoA′*-2	This work
CP1021	CP1017 *xylR1*::Tn*phoA′*-7	This work
CP1022	CP1018 *xylR1*::Tn*phoA′*-7	This work
CP1023	W3110 *minA*::*aph xylR1*::Tn*phoA′*-2	This work
CP1024	CP1018 *xylA1*::Tn*phoA′*-7	This work
CP1025	CP1014 Φ(P_A-*lac*)	This work
CP1026	CP1014 Φ(P_A-*lac*) *xylG1*::Tn*phoA′*-7	This work
CP1027	CP1014 Φ(P_A-*lac*) *xylR1*::Tn*phoA′*-7	This work
CP1028	CP1014 Φ(P_F-*lac*)	This work
CP1029	CP1014 Φ(P_F-*lac*) *xylG1*::Tn*phoA′*-7	This work
CP1030	CP1014 Φ(P_F-*lac*) *xylR1*::Tn*phoA′*-7	This work
W3110	Prototroph	B. Bachmann
Plasmids		
pACYC184	*ori* (p15A) Tc^r Cm^r	Pharmacia
pBluescript SKII(+)	*ori* (pMB1) Ap^r	Stratagene
pBR322	*ori* (pMB1)Ap^r Tc^r	Lab collection
pGEM7zf(+)	*ori* (pMB1) Ap^r	Promega
pKK232-8	*ori* (pMB1) *′cat* Ap^r	Promega
pRS550	*ori*(pMB1) *′lacZ* Ap^r Km^r	41
pRS551	*ori*(pMB1) *′lacZ* Ap^r Km^r	41
pSK131	pBluescript SKII(+) *′tnp* Ap^r	This work
pSK223	pSK131 P_{xyl}	This work
pSK239	pSK131 *xylFGHR*	This work
pSK256	pGEM7zf(+) *xylHR* Ap^r	This work
pSK258	pSK256 *xylR*::*tet* Ap^r	This work
pSK274	pBR322 *xylFGHR* Ap^r	This work
pSK331	pTrc99A *xylR* Ap^r	This work
pSK335	pACYC184 P_{xyl} Ap^r	This work
pSK363	pKK232-8 P_R-*cat* Ap^r	This work
pTrc99A	*ori* (pMB1) P_{trc} Ap^r	Pharmacia

associating with other components in the transcriptional apparatus.

MATERIALS AND METHODS

Bacterial strains, growth conditions, and media. *E. coli* K-12 strains used in this study are listed in Table 1. Cells were grown with shaking at 37°C unless otherwise stated. The medium used was either LB (10 g of tryptone, 5 g of yeast extract, and 5 g of NaCl per liter) or M9 minimal salts medium (27), both of which were solidified by the addition of 1.5% agar (Difco). Carbon sources were 0.2% each glycerol, D-xylose, and D-glucose. Supplements, when required, were added at the following concentrations: ampicillin, 50 μg/ml; kanamycin, 20 μg/ml; tetracycline, 15 μg/ml; and chloramphenicol, 20 μg/ml. Growth was monitored with a Beckman model DU-65 spectrophotometer.

DNA manipulation. Methods for plasmid, chromosomal, and bacteriophage λ DNA purifications were described previously (36). Restriction endonuclease digestion and ligation with T4 DNA ligase were carried out as recommended by the manufacturer (Boehringer Mannheim Biochemicals). All sequencing reactions were performed with DNA Sequenase version 2.0 (U.S. Biochemical Corp.). The oligonucleotides used in primer extension reactions were XA (CG AACGCGATCGAGA), complementary to codons 6 to 13 of *xylA*; XF (CAGG AGTGAGGTGCAAAGGG), complementary to codons 9 to 15 of *xylF*; and XR (CGCCTTCTACTACCTGCCGG), complementary to codons 19 to 26 of *xylR*. Two synthetic oligonucleotides were used for the cloning of *xylR*, one corresponding to codons 1 to 7 (XRN; CCGGATCCATGTTTACTAAACGTCACC) with an additional *Bam*HI recognition sequence and the other complementary to codons 386 to 392 (XRC; CCAAGCTTCAACATGACCTCGCTATTT) with an additional *Hin*dIII recognition sequence. These oligonucleotides were annealed to pSK274 and PCR amplified (30 cycles at 72°C with the Perkin-Elmer GeneAmp PCR system 2400) by *Taq* polymerase to obtain the DNA fragment containing *xylR*. The PCR product was digested with *Bam*HI and *Hin*dIII and was inserted into an expression vector, pTrc99A, linearized with the same enzymes. The *xylR* sequence of the resulting plasmid, named pSK331, was confirmed by DNA sequencing. Plasmid pSK335 was constructed by cloning the *Sac*II/*Hae*III fragment (332 bp) of the *xyl* promoter region (P_{xyl}) located between *xylA* and *xylF* into the *Bam*HI/*Hin*dIII site of pACYC184 by using a linker (45 bp). To create *lacZ* promoter fusions, the DNA fragments (332 bp from pSK335) containing the region for P_A and P_F were cloned into the *Eco*RI site of pRS551, a *lacZ* operon fusion plasmid (41), followed by characterizations of two different fusions, P_A-*lacZ* and P_F-*lacZ*. The P_R-*lacZ* fusion was constructed by inserting the *Nru*I/*Nsi*I fragment (805 bp) containing the promoter from pSK256 into pRS550. Plasmid pRS550 is the same as pRS551 except that the order of *Bam*HI and *Eco*RI sites is reversed.

Genetic procedures. The P1*vir* transducing phage was used for the transduction experiments (27). Transposon mutagenesis was performed with strain CP1014 and λ::Tn*phoA′*-1, generating an insertion (Kan^r) or a transcriptional fusion to *lacZ* as described previously (48). Mutagenized cells with λ::Tn*phoA′*-1 were plated on 0.2% glycerol M9 medium. Tn*phoA′*-1 insertions, when needed to change an antibiotic resistance or to remove the *lacZ* gene, were recombinationally swapped with Tn*phoA′*-2 carrying *tet* and *lacZ* genes or with Tn*phoA′*-7 carrying only the *cat* gene. All promoter *lacZ* fusions were inserted into the chromosome by using lambda phage RS45, in which the copy number of prophage carrying the promoter fusions was confirmed by PCR (31).

β-Galactosidase assay. Cells were grown in 0.2% glycerol M9 medium supplemented with 0.2% D-xylose, 0.2% D-xylose plus D-glucose, or no sugar to an optical density at 600 nm (OD_{600}) of 0.4 to 0.6. β-Galactosidase activity was monitored by the method of Miller (27). All data were averaged from at least three independent experiments. Standard deviations of values presented were not more than ±5%.

Uptake assay for D-[^{14}C]xylose. Transport of D-[^{14}C]xylose was measured by harvesting mid-log-phase cells grown in glycerol M9 media supplemented with 0.2% D-xylose, washed three times with 10 volumes of 10 mM potassium phosphate buffer (pH 7.0), and then resuspended in the same buffer to adjust the final OD_{600} to 0.2. D-[^{14}C]xylose (91 mCi/mmol; Amersham Corp.) was added at 2 μM

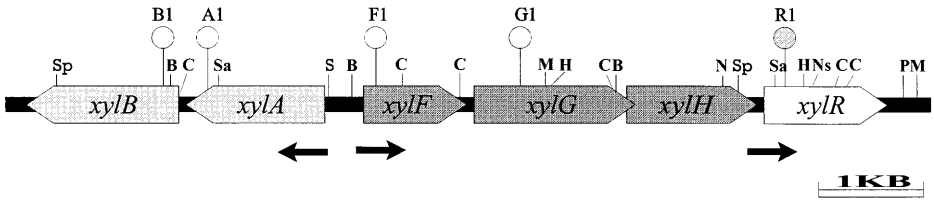

FIG. 1. Organization of the *xyl* locus. The genes *xylAB* encoding metabolic enzymes are light gray; the transport components *xylFGH* are dark gray. The *xylR* gene is involved in transcriptional regulation of the *xyl* genes. The circles represent transposon insertions with transcriptional fusion to *lacZ* (open) or not (filled). The arrows below the diagram indicate the transcriptions from P_A, P_F, and P_R revealed by this study. Restriction enzyme sites: B, *Bgl*II; C, *Cla*I; H, *Hpa*I; M, *Mlu*I; N, *Nru*I; Ns, *Nsi*I; P, *Pvu*II; S, *Sac*II; Sa, *Sal*I; Sp, *Sph*I.

to a 5-ml cell suspension, and the mixture was further incubated. A 1-ml sample was taken at 10, 20, 40, and 60 s and filtered through a 0.45-μm-pore-size nitrocellulose filter (Amicon). After drying, radioactivities were counted (6).

In vivo cloning of chromosomal junction of transposon insertions. Plasmid pSK131 (3,655 bp), used for cloning a junction of transposon insertions, is a version of pBluescript SKII(+) lacking the *lac* region, which contains the *Pvu*II/*Hpa*I fragment (1,238 bp) of the transposase gene from λ::Tn*phoA′*-1. The plasmid carries an extra multicloning site from pGEM7zf(+) inserted into the N-terminal side of the transposase gene. To pick up an insertional junction, a transposon insertion was transferred from a *xyl* mutant to CP367/pSK131 [*polA*(Ts)]. The strain was grown at 42°C to promote a homologous recombination between the transposase genes (30). Chromosomal DNA from the pSK131-integrated cells was digested with an appropriate restriction endonuclease recognizing the multicloning site of pSK131 and ligated with T4 DNA ligase before transformation. A clone that contained a chromosomal DNA fragment flanking the transposon insertion was recovered and sequenced by using a primer (GG CGGCGACGTTAACCAAGC) complementary to the C-terminal portion of the transposase gene. The sequence was subjected to analysis with the BLAST database search. The same technique was used to obtain pSK223 (the *xyl* promoter region) and pSK239 (*xylFGHR*) from strains CP1015 [*polA*(Ts)] and CP1016 [*polA*(Ts)] containing *xylA3*::Tn*phoA′*-1 and *xylA2*::Tn*phoA′*-1 insertions, respectively. The *xylA2*::Tn*phoA′*-1 and *xylA3*::Tn*phoA′*-1 insertions occurred right after the 18th and 1,265th bases from the translational start of the *xylA* gene with reverse orientations of *lacZ* relative to *xylA* transcription. Plasmids pSK223 and pSK239 were recovered from the chromosomally integrated pSK131 by *Cla*I (1,982 bp of P_{xyl}) and *Sma*I (9,634 bp of *xylFGHR*) digestions, respectively. The *xylFGHR* genes (5,746 bp) from pSK239 were subcloned into pBR322 (*Eco*RV/*Sal*I) by *Xho*I/*Pvu*II digestions to generate pSK274. The *xylHR* genes (3,064 bp from pSK239) were inserted into pGEM7zf(+), using the *Bgl*II/*Mlu*I enzymes, yielding pSK256. To construct pSK258, the *tet* gene (1,444 bp) was inserted into the *xylR* gene of pSK256 after deletion of the *Sal*I/*Hpa*I fragment of *xylR*.

Minicell labeling with [^{35}S]methionine. Plasmid pBR322 or pSK274 containing the *xylFGHR* genes was transformed into the minicell-producing strain CP1023 carrying *xylR*::Tn*phoA′*-2. Minicells were prepared and incubated with [^{35}S]methionine (0.2 μM, 30 μCi/mmol) for 1 h (13). Proteins were precipitated with 5% trichloroacetic acid and were harvested by centrifugation. The pellets were then washed with 10 mM Tris-acetate (pH 7.4) and analyzed by sodium dodecyl sulfate (SDS)–12% polyacrylamide gel electrophoresis (18). After staining with Coomassie blue R-250, the gel was subjected to autoradiography.

Primer extension analysis. To determine the P_A and P_F transcriptional sites, total cellular RNAs were prepared from CP1014/pSK223 containing the promoter region between *xylA* and *xylF*. Cells were grown in 0.2% glycerol M9 medium supplemented with 0.2% xylose, 0.2% each xylose and glucose, or no sugar and were harvested at an OD_{600} of 0.5 by centrifugation. After freezing for 5 h at −70°C, the samples were thawed at room temperature, and total RNAs were isolated with RNAzol (Cinna/Biotex, Friendwood, Tex.). Primer extension reactions were performed as described previously (15), with the following modifications. The primers XA and XF (10 pmol of each) were labeled with [γ-^{32}P]ATP and T4 polynucleotide kinase. Total cellular RNA (20 μg) was mixed with 10 ng of [γ-^{32}P]ATP-labeled primer and annealed in hybridization buffer (1 M NaCl, 1 mM EDTA, 160 mM HEPES [pH 7.5]). The reaction mixture contained 1 mM deoxynucleoside triphosphate mixture, 50 mM Tris-HCl (pH 8.3), 7 mM $MgCl_2$, 40 mM KCl, 1 mM dithiothreitol, 0.1 mg of bovine serum albumin per ml, and 10 U of avian myeloblastosis virus reverse transcriptase. The mixtures were incubated at 42°C for 45 min, followed by extraction with phenol and precipitation with ethanol. The samples were then resuspended in 10 μl of TE (10 mM Tris HCl, 1 mM EDTA [pH 8.0]) and added to 2 volumes of loading buffer (95% formamide, 25 mM EDTA, 0.05% bromophenol blue, 0.05% xylene cyanol). The cDNAs synthesized were separated by electrophoresis on a 6% sequencing gel. The size markers were generated by a reaction with the same primer. To determine the P_R start site, CP1014/pSK363 was grown in 0.2% glycerol M9 minimal medium to late log phase, and total cellular RNA was isolated. pSK363 has a DNA insert (*Nru*I/*Nsi*I fragment of 805 bp from pSK256 with appropriate linkers) containing P_R in the multiple cloning site (*Bam*HI and *Hin*dIII) of pKK232-8 such that the insert was surrounded by the two transcriptional terminators *rrnBT1* and *rrnBT2* to prevent a possible readthrough from any region of the vector. The primer XR was used for primer extension.

Gel mobility shift assay. Strain CP1020 containing pSK258 (*xylR*::*tet*) or pSK256 (*xylR*$^+$) was grown to late log phase (OD_{600} of 0.8) in 0.2% glycerol M9 medium containing ampicillin (30 μg/ml). Cells were harvested by centrifugation

TABLE 2. Phenotypes of insertions in *xyl* structural genes

Allele	Location[a]	Orientation[b]	Xylose growth[c]	Uptake (nmol/mg/min)[d]
xyl$^+$ (CP1014)	NA[e]	NA	+++++	281.88 (100)
xylA1::Tn*phoA′*-1	1119	+	−	89.46 (31.7)
xylB1::Tn*phoA′*-1	119	+	−	220.68 (78.3)
xylF1::Tn*phoA′*-1	40	+	+++	ND[f]
xylG1::Tn*phoA′*-1	368	+	+++	9.92 (3.5)
xylR1::Tn*phoA′*-1	171	−	−	1.62 (0.6)

[a] A position just before the insertion was counted from the first base of the initiation codon of the mutated gene.

[b] The orientation of *lacZ* is indicated as the same as (+) or the opposite of (−) the orientation of transcription.

[c] Growth on a 0.2% xylose minimal plate was assessed in the CP1014 background after incubation for 2 days at 37°C. The plus and minus signs represent relative levels of growth.

[d] A mid-log-phase culture grown in M9 minimal medium containing 0.2% glycerol and 0.2% D-xylose was used as described in Materials and Methods. Percent uptake rates are in parentheses.

[e] NA, not applicable.

[f] ND, not determined.

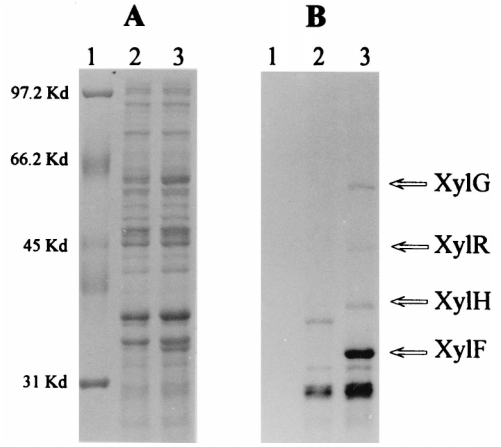

FIG. 2. Identification of protein products from *xylFGH* and *xylR* genes. To identify the xylose high-affinity transporters XylFGH and the regulator XylR, minicells harboring plasmid pBR322 or pSK274 were isolated and analyzed by labeling with [^{35}S]methionine and SDS–12% polyacrylamide gel electrophoresis as described in Materials and Methods. The Coomassie blue-stained gel (A) and its autoradiogram (B) are shown. Minicells contain plasmids pBR322 (lane 2) and pSK274 (lane 3). Lane 1, protein size markers. The arrows indicate the labeled Xyl polypeptides.

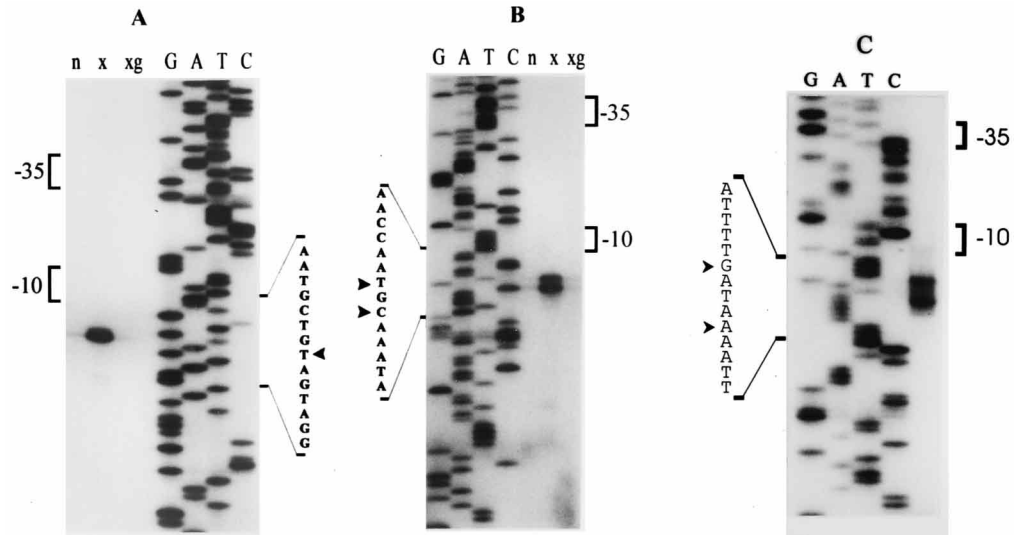

FIG. 3. Determination of transcription initiation sites by primer extension analysis. Lanes G, A, T, and C show the sequencing ladders with primers labeled at 5′ positions by T4 polynucleotide kinase. The −35 and −10 regions are marked. The extended primers are shown in the first three lanes of panel A (P_A), the last three lanes of panel B (P_F), and the last lane of panel C (P_R). Cells were grown in 0.2% glycerol M9 medium with no supplement (n) or supplemented with 0.2% xylose (x) and 0.2% xylose plus 0.2% glucose (xg), and total RNAs were isolated from strain CP1014/pSK223 containing P_A and P_F and from CP1014/pSK363 for P_R. The complementary DNAs were synthesized by avian myeloblastosis virus reverse transcriptase with 20 μg of total RNA and 10 ng of labeled primer. The arrowheads indicate the positions of 5′ ends of complementary DNA synthesized from the RNA transcripts for P_A, P_F, and P_R.

(5,000 × *g*) for 10 min, resuspended in a 1/20 volume of 50 mM Tris-HCl (pH 7.9)–30 μM dithiothreitol, and sonicated in ice. The mixture was then centrifuged to remove the insoluble fraction. The protein concentration of the soluble fraction was adjusted to 1 μg/μl (22), and that fraction was aliquoted for storage at −20°C. The *xyl* promoter region (332 bp from the *Sac*II-to-*Hae*III site) is contained in pSK335. The fragment from pSK335 was dephosphorylated with calf intestinal phosphatase and labeled with [γ-^{32}P]ATP by T4 polynucleotide kinase. The assay was carried out (51) in a 20-μl solution containing 20 mM Tris-HCl (pH 7.9), 50 mM KCl, 1 mM EDTA, 1 mM dithiothreitol, and 10% glycerol with crude extract of 0.5 to 10 μg of protein mixed with 1 ng of the radiolabeled *xyl* promoter DNA and 1 μg of sonicated salmon sperm DNA as a competitor. The reaction mixtures were not supplemented or supplemented with 13.3 mM xylose, incubated for 20 min at 25°C, and subjected to electrophoresis on a 5% polyacrylamide gel with 0.5× TBE (1× TBE is 90 mM Tris-borate [pH 8.3] and 2.5 mM EDTA) buffer at room temperature. The gels were exposed to X-ray film (Kodak) at −70°C.

In vivo footprinting with DMS. Plasmid pSK335 was transformed into CP1022 (*xylR1*::Tn*phoA′*-7 *xylG1*::Tn*phoA′*-1) containing *xylR* plasmid pSK331 with extensions of nine and seven amino acids from expression vector pTrc99A on the N and C termini, respectively. The XylR protein expressed was active in DNA binding as measured by β-galactosidase activities from *xylG1-lacZ* in a *xylR*-negative background. β-Galactosidase expression was also inducible by xylose and was catabolite repressible (data not shown). Cells were grown to early log phase in 0.2% glycerol M9 medium and mixed with 1 mM isopropyl-β-D-thiogalactopyranoside (IPTG). After induction for 1 h, the culture was further incubated for 30 min with or without xylose and then treated with dimethyl sulfate (DMS) as described previously (25, 46). The pSK335 DNA was purified, digested with *Bam*HI for the top strand or with *Hin*dIII for the bottom strand, dephosphorylated with calf intestinal phosphatase, and labeled with [γ-^{32}P]ATP. The labeled DNA was further digested with the second enzyme *Hin*dIII for a *Bam*HI digest, or vice versa. A DNA fragment with methylated guanine was purified by agarose gel electrophoresis and treated with 1 M piperidine at 90°C for 45 min (26). The reaction mixtures were lyophilized and then solubilized in gel loading buffer. The modification patterns were analyzed on a 6% sequencing gel.

RESULTS

Characterization of *xyl* genes by transposon insertions. Using Tn*phoA′*-1 containing *lacZ*, we generated in CP1014, an *E. coli* K-12 strain, random insertions that resulted in various degrees of growth defects on D-xylose. Among 58 insertions screened, 50 were linked to the *xyl* locus at 80 min, with more than 90% of the cotransduction frequencies measured by phage P1. Some of the insertions were isolated by their properties of enhancing growth on other pentoses (44). We located 30 insertions in the *xyl* region by cloning and sequencing of the flanking regions of insertions, using plasmid pSK131 integrated into the translocation sites (Materials and Methods). Two types of insertions, causing a structural or regulatory defect, were characterized to elucidate the organization and regulation of the *xyl* operon. One class of insertions found in most of the structural genes *xylA*, *xylB*, *xylF*, *xylG*, and *xylR* is described in Fig. 1 and Table 2. A total of eight other insertions were located in the promoter region of the *xyl* operon, which will be described later. As expected, strains with insertions in *xylA* and *xylB* did not grow on D-xylose, although they transport D-xylose at the wild-type level (Table 2). Strains with a *xylF* or *xylG* insertion still grew on D-xylose, albeit less efficiently. However, their uptake rates were dramatically reduced, indicating that they are involved in high-affinity transport. Interestingly, a *xylR* mutation affected both growth and transport of D-xylose, and the transport defect was even more severe than that of a *xylG* mutant, presumably due to an involvement of XylR in the regulation of the low-affinity transporter (XylE).

Proteins expressed from the *xylFGHR* operon were characterized in minicells, derived from CP1023, containing plasmid pSK274 or pBR322. Polypeptides encoded from the plasmids were labeled with [^{35}S]methionine and analyzed by SDS-polyacrylamide gel electrophoresis (Fig. 2). Plasmid pSK274 produced four distinct bands not present in pBR322. The smallest one, with an M_r of 36,000 (35,734 predicted), was also seen on a Coomassie blue-stained gel and appears to be XylF (the xylose-binding protein). Others were found to have the following estimated M_rs: XylH, 41,030; XylR, 44,869; and XylG, 56,470.

Transcription initiation at the P_A and P_F promoters. The spacing of 365 bp between the two *xyl* gene clusters implies the existence of at least two promoters, here called P_A and P_F, directing transcription from *xylA* and *xylF*, respectively. Sites of transcription initiation in P_A and P_F were determined by primer extension for the transcripts from CP1014/pSK223 grown in the presence of 0.2% D-xylose (alone or plus glucose)

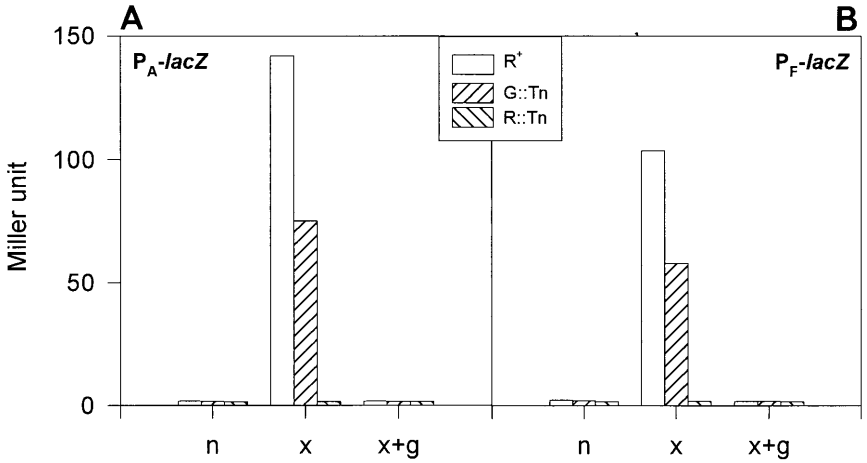

FIG. 4. Effects of *xyl* insertions on the expressions of P_A (A) and P_F (B). To examine effects of sugars or *xyl* mutations on P_A expression, lambda prophage containing the P_A-*lacZ* fusion was used as in CP1025 (*xylR*$^+$ P_A-*lac*; R^+), CP1026 (*xylG1*::Tn*phoA′*-7 P_A-*lacZ*; G::Tn), and CP1027 (*xylR1*::Tn*phoA′*-7 P_A-*lac*; R::Tn). Expression of P_F was observed in CP1028 (*xylR*$^+$ P_F-*lacZ*; R^+), CP1029 (*xylG1*::Tn*phoA′*-7 P_F-*lacZ*; G::Tn), and CP1030 (*xylR1*::Tn*phoA′*-7 P_F-*lacZ*; R::Tn) grown in 0.2% glycerol M9 minimal medium containing no sugar (n), 0.2% xylose (x), and 0.2% xylose plus 0.2% glucose (x+g). Samples were taken from mid-log phase to monitor β-galactosidase activity as described in Materials and Methods.

or the absence of sugar. As shown in Fig. 3A, one major band was obtained for P_A with any RNA sample, indicating transcription from 42 nucleotides upstream of the site of *xylA* translation initiation. However, an experiment with P_F gave two major bands, indicating two possible initiations from 60 and 62 nucleotides upstream of the translation start (Fig. 3B). The transcriptions at both P_A and P_F were xylose inducible and catabolite repressible, always occurring at the same positions in any tested conditions.

XylR acts as a positive regulator. To analyze gene expression from P_A and P_F, transcriptional fusions to *lacZ* were constructed (Materials and Methods). The expression of P_A was enhanced about 70-fold by D-xylose and substantially reduced by an addition of glucose (Fig. 4A). The P_F transcription was regulated in a similar manner, with more than 50-fold induction (Fig. 4B). An insertion (Tn*phoA′*-7) in *xylG* ameliorated the induction fold, perhaps due to its polarity with respect to downstream *xylR*. However, an insertion in *xylR* completely abolished transcription. The *xylR*-containing plasmids pSK256, pSK274, and pSK331, but not pSK258 (*xylR*::*tet*), were able to complement the *xylR* insertion and restored the wild-type patterns of P_A and P_F regulation (data not shown). It was observed that the expression levels were slightly higher with the multicopy *xylR*. The results suggest that the *xylR* gene serves as a positive regulator for both operons and that it has its own promoter downstream of the *xylG* insertion.

P_R, a secondary promoter for *xylR*. To localize the P_R promoter, three DNA segments comprising the region between the *xylG1* insertion and the *xylR* gene were tested for the ability to initiate transcription by inserting them into the promoter-probing vector pRS551 (′*lacZ*). Expression of β-galactosidase was detected only with the *Nru*I/*Nsi*I fragment (805 bp) containing the 3′ region of *xylH* and the 5′ region of *xylR*. For this region, primer extension analysis was carried out with pSK363 (Materials and Methods), indicating initiations of P_R at 69 and 73 bases upstream from the *xylR* start codon (Fig. 3C). The P_R promoter has the −10 (TTCTTG) and −35 (TGGACT) regions with 16-bp spacing, showing a poor similarity to the σ^{70} consensus. The regulation of P_R was investigated by using the promoter fusion to *lacZ* inserted into the chromosome. The promoter has a low-level expression (about 10%) compared to that of P_F, although the activity is increased considerably after mid-log phase (data not shown), which was not affected by glycerol, xylose, or glucose.

Binding of XylR to the P_A and P_F promoters. For mobility shift assay (51), crude extracts were prepared from strain CP1020 (*xylR*) containing pSK258 (*xylR*::*tet*) or pSK256 (*xylR*$^+$). The target DNA (332 bp in pSK335) was the *Sac*II/*Hae*III fragment of the *xyl* promoter region. D-Xylose enhanced the binding of XylR to the target DNA, which is proportional to the XylR concentration (Fig. 5). A minor shift in gel mobility was observed without xylose, and there is a hint of retardation even in the absence of both XylR and xylose. It is possible that unliganded XylR and some other DNA-binding protein(s) may associate with this region. Indeed, a band shift was observed after addition of cyclic AMP (data not shown).

The binding of XylR to the promoter region was initially

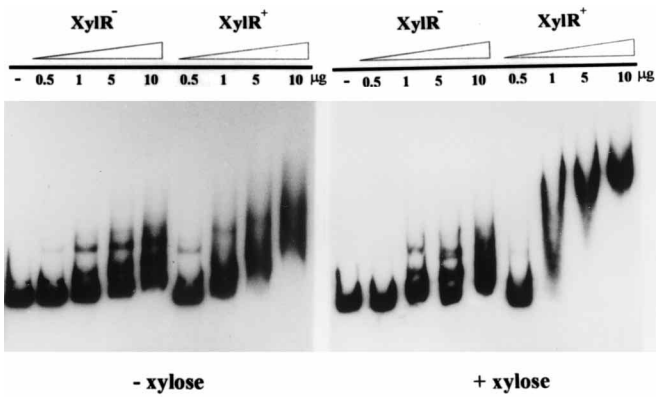

FIG. 5. Gel mobility shift with XylR. The assay was performed with a 332-bp DNA (*Sac*II/*Hae*III fragment as in Fig. 7) containing P_A and P_F and with cell extracts from CP1020/pSK258 (XylR$^-$) and CP1020/pSK256 (XylR$^+$). End-labeled DNAs generated by T4 polynucleotide kinase were mixed with 0.5, 1, 5, or 10 μg of crude extract without (left) or with (right) 13.3 mM xylose. The reaction mixtures were subjected to a 5% polyacrylamide gel electrophoresis in the absence (left) or presence (right) of 13.3 mM xylose, followed by autoradiography. The leftmost lane in each panel contains no protein, and the others contain the indicated amounts of total soluble proteins.

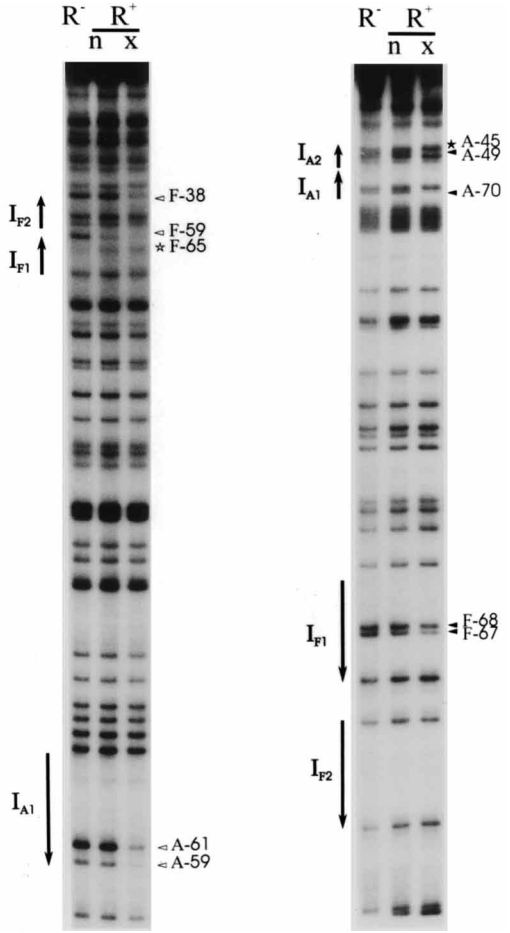

FIG. 6. In vivo DMS footprinting of the *xyl* promoter regions for both strands. After induction of *xylR* with IPTG, CP1022/pSK335 with pTrc99A (*xylR*$^-$; R$^-$) or with pSK331 (*xylR*$^+$; R$^+$) was treated with DMS in the absence (n) or presence (x) of xylose. Methylation patterns of the *xyl* regulatory region in pSK335 were analyzed as described in Materials and Methods. The arrowheads indicate bases protected, and the stars represent enhanced methylation sites. Open and closed symbols represent the top and bottom strands, respectively. The numbers on the right designate bases counted from the +1 position of the mRNA start site of P_A (A) or P_F (F).

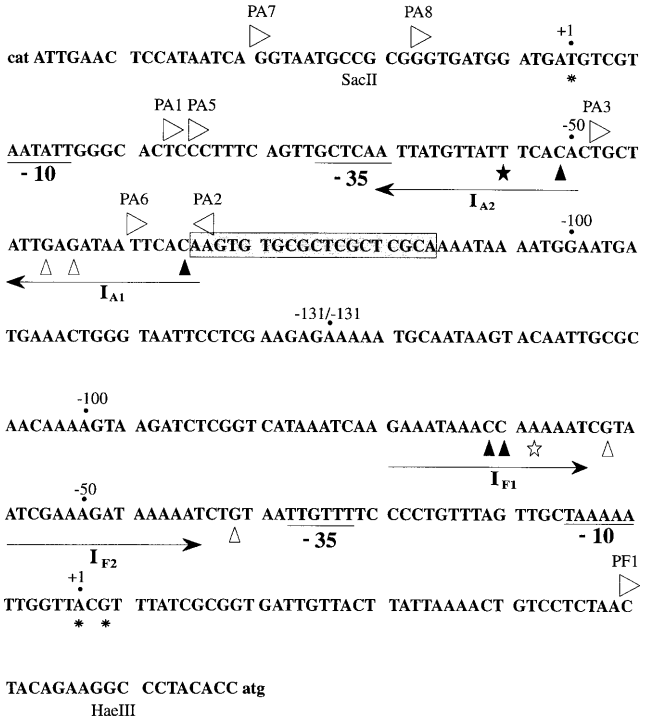

FIG. 7. Nucleotide sequence of the *xyl* promoter region with various regulatory sites. Initiation codons for *xylA* and *xylF* are located at the start and the end. The −10 and −35 regions of two outwardly directed promoters, P_A and P_F, are underlined, and the transcription start sites are marked by asterisks. Transposon insertions obtained in this region are shown above the sequence, with the orientation of *lacZ* as indicated. The putative CRP-binding consensus sequence is boxed. Guanine bases protected by XylR have reduced intensities (arrowheads). The bases with enhanced intensities are also marked (stars). Open and closed symbols represent the protected bases on the top and bottom strands, respectively (Fig. 6). The direct repeat sequences are marked by arrows.

attempted with purified XylR protein, which turned out to be unsuccessful due to a loss of DNA-binding activity of the purified XylR. Thus, we performed in vivo footprinting (46) with XylR overproduced from pSK331. Cells carrying pSK331 (*xylR*$^+$) and pSK335 (P_{xyl}, the *xyl* promoter region) were treated with DMS in the presence or absence of D-xylose, generating a reproducible pattern of methylated and unmethylated guanines in the *xyl* regulatory region (Fig. 6). Before the DMS treatment, amounts of XylR expressed were confirmed by Western analysis with anti-XylR antiserum to be similar in induced and uninduced conditions (data not shown). Without XylR, there is no change in DMS modification regardless of the presence of inducer (data not shown). As shown in Fig. 6, guanine residues at positions A-59, A-61, F-59, and F-38 on the top strand and at positions A-49, A-70, F-68, and F-67 on the bottom strand were protected by XylR from methylation upon xylose induction. The bases were counted from either the *xylA* (A) or *xylF* (F) transcription start site. Two hotspots, A-45 and F-65, with increased densities were observed, indicating that there are two regions in the *xyl* promoters (Fig. 7) occupied with XylR. One region (I_A) is located between −35 and the CRP consensus sequence of the promoter P_A. The other (I_F) is located a little upstream of the P_F promoter (−35). Each of the XylR-binding regions contains a direct repeat, comprising about four helical turns of DNA. When there is no inducer, only two positions of I_{F1}, F-59 and F-65 (hotspot), showed modifications on the top strand, suggesting that XylR protein interacts with the region under this condition. Although only a minor shift was observed with unliganded XylR by mobility shift assay, the footprinting assay clearly demonstrated that XylR binds to I_{F1} in both induced and uninduced conditions and that three half sites, I_{F2}, I_{A1}, and I_{A2}, were occupied under induced conditions.

DISCUSSION

We have characterized the functions and regulation of the genes involved in the uptake and metabolism of xylose. As expected from the sequence similarities, the transport of xylose involves the three essential components (XylFGH) of the binding-protein-mediated transport system that shares homologies with other ABC (ATP-binding cassette)-type transporters classified as the AraH family (38). A mutation among these genes eliminates an activity of the high-affinity uptake while still maintaining an ability to utilize xylose (Table 2), perhaps through the low-affinity system (XylE) that was characterized previously (6). These genes, together with *xylAB*, are positively regulated by the same protein (XylR [Fig. 4]), which appears to recognize the consensus sequences located in their promoter

TABLE 3. Growth and expression of the promoter insertions

Insertion	Xylose (0.2%)[a]	*xylA1-lacZ* expression[b] (uninduced/induced)	Location
PA7	−	12/8	+25 from P_A start
PA8	−	10/12	+13 from P_A start
PA1	−	11/12	−17 from P_A start
PA5	−	ND[c]	−19 from P_A start
PA3	+	30/28	−51 from P_A start (I_{A2})
PA6	++	ND	−65 from P_A start (I_{A1})
PA2	++	50/45	−72 from P_A start (CRP-binding site)
PF1	+++	9/340	+42 from P_F start

[a] Growth was assessed in the CP1014 background after incubation for 3 days at 37°C. Measurement of colony size was arbitrary such that a single + is roughly equivalent to 1 mm in diameter. During the period, all strains showed the same level of growth on glucose medium.

[b] Expression of the *xylA1*::Tn*phoA′*-1 fusion (Kan^r) was monitored under uninduced and induced conditions in strains containing promoter insertions with Tn*phoA′*-7 (*cat*). Cells were grown in 0.2% glycerol M9 minimal medium with 0.2% xylose (induced) or without the sugar (uninduced). Activities of β-galactosidase shown in Miller units were assayed from cells at late log phase and averaged from four independent experiments.

[c] ND, not determined.

regions. For the *xylAB* and *xylFGH* promoters, these sequences were probed by direct binding in vitro with XylR, whereas the same consensus sequence in the *xylE* promoter was found merely by prediction. No sequence similarity was detected in the region for the internal promoter P_R specific for *xylR*.

The two XylR-binding sites (I_A and I_F) found in the *xyl* promoters are located adjacent to the RNA polymerase-binding sites (Fig. 7), each spanning 36 to 37 bp (about four helical turns) with a direct repeat. A consensus sequence, ---gaAa-a--a-AAT, presumably for the binding of monomeric XylR emerges from the comparison of the four half sites (I_{A1}, I_{A2}, I_{F1}, and I_{F2}) that are rich in adenines. The capitalized bases are found in all four sequences while the lowercase bases match three of four. Despite the presence of a consensus, a similarity in a pair of half sites is more prominent. It is likely that XylR binds as a dimeric form, each molecule occupying two helical turns of each half site as in AraC (2, 23) or as in other helix-turn-helix proteins (1) such as cI (16) and Cro (49). Interestingly, the conserved bases in each half site, both in I_A and in I_F, are repeated with a periodicity of 20 or 21 bp (about two helical turns), suggesting that the contacts of each XylR monomer occur on the same side of the DNA surface. In this regard, XylR is similar to other members of the AraC family regulators that bind to direct repeat structures with a gap of 4 bp, spanning about four helical turns as a whole (23). On the other hand, some regulators of the same family, including RhaS and RhaR, recognize an inverted repeat with a gap of 16 or 17 bp (8).

A similarity of XylR protein to other AraC family proteins whose DNA-binding motifs are organized as two helix-turn-helix (HTH) structures lies in the COOH-terminal portion of the peptide as for other proteins in the group (9, 45). Also, it has been reported that the second helix of the HTH contacts a target site (2), whereas the N-terminal region of this family, which is presumed to contain a binding site for an effector that confers a specificity, is nonhomologous. The predicted DNA-binding domain of XylR contains two HTH structures in the C-terminal region, comprising 304 to 323 and 353 to 372 amino acid residues.

The regulation of transcription in the *xylAB* and *xylFGH* operons must involve interactions of each promoter with XylR, CRP, and RNA polymerase. The close proximity between the XylR-binding site, both in I_A and in I_F, and the site for RNA polymerase suggests a direct protein interaction between XylR and RNA polymerase. We obtained transposon insertions in the promoter regions (Fig. 7; Table 3) that cause severe defects in xylose utilization. Growth of strains with these insertions scored after several days on D-xylose minimal plates, together with the reporter expressions of *xylA*, clearly distinguished the insertional phenotypes from one location to another. The insertions in the region for RNA polymerase interaction (*xylPA1* and *xylPA5*) or downstream from it (*xylPA7* and *xylPA8*) never grew on xylose plates, whereas the insertions in the proposed XylR-binding sites (*xylPA3* and *xylPA6*) and in the predicted CRP-binding site (*xylPA2*) exhibited a leaky phenotype on D-xylose. It was also noted that the growth of the *PA3* insertion was a little slower than that of *PA6* and *PA2*. These results are consistent with the locations of various regulatory sites proposed and imply an involvement of CRP and XylR in P_A activation. Growth of the *xylPF1* insertion was basically indistinguishable from that in either *xylF* or *xylG*, indicating a defect in the high-affinity transport.

Although it is evident that transcription of the *xyl* promoters is activated by D-xylose, we cannot rule out the possibility of a transcriptional repression in the absence of an inducer, as in the case of the *araBAD* operon that is negatively regulated by AraC and DNA looping. It is conceivable from the physiological point of view that the transcription of *xyl* genes is maintained at a repressed level in the absence of D-xylose. We observed that there is a slight elevation of the *xylG-lacZ* transcription in both noninduced and induced conditions by the insertions of *xylPA1*, *xylPA2*, and *xylPA3* (44). This may imply that the P_A region somehow forms a higher-ordered structure with the P_F region and may negatively affect gene expression.

ACKNOWLEDGMENTS

This work was supported in part by grant KOSEF 96-0401-01-01-3 from the Korea Science and Engineering Foundation.

We thank A. Schneider for reading the manuscript and R. W. Simons and B. Wanner for kindly providing plasmids and phages.

REFERENCES

1. **Brennan, R. G., and B. W. Matthews.** 1989. The helix-turn-helix DNA binding motif. J. Biol. Chem. **264:**1903–1906.
2. **Brunelle, A., and R. Schleif.** 1989. Determining residue-base interaction between AraC protein and *araI* DNA. J. Mol. Biol. **209:**607–622.
3. **Carra, J. H., and R. Schleif.** 1993. Variation of half site organization and DNA looping by AraC protein. EMBO J. **12:**35–44.
4. **Casadaban, M. J.** 1976. Regulation of the regulatory gene for the arabinose pathway, *araC*. J. Mol. Biol. **104:**556–557.
5. **David, J. D., and H. Wiesmeyer.** 1970. Control of xylose metabolism in *Escherichia coli*. Biochim. Biophys. Acta **201:**497–499.
6. **Davis, E. O., and P. J. F. Henderson.** 1987. The cloning and DNA sequence of the gene *xylE* for xylose-proton symport in *Escherichia coli* K-12. J. Biol. Chem. **262:**13928–13932.
7. **Dunn, T., S. Hahn, and R. Schleif.** 1984. An operator at −280 base pairs that is required for repression of *araBAD* operon promoter: addition of DNA

helical turns between the operator and promoter cyclically hinders repression. Proc. Natl. Acad. Sci. USA **81:**5017–5020.
8. **Egan, S. M., and R. F. Schleif.** 1994. DNA-dependent renaturation of an insoluble DNA binding protein: identification of the RhaS binding site at *rhaBAD*. J. Mol. Biol. **243:**821–829.
9. **Gallegos, M.-T., C. Michan, and J. L. Ramos.** 1993. The XylS/AraC family of regulators. Nucleic Acids Res. **21:**807–810.
10. **Hahn, S., T. Dunn, and R. Schleif.** 1984. Upstream repression and CRP stimulation of the *Escherichia coli* L-arabinose operon. J. Mol. Biol. **180:**201–204.
11. **Hamilton, E. P., and N. Lee.** 1988. Three binding sites for AraC protein are required for autoregulation of *araC* in *Escherichia coli*. Proc. Natl. Acad. Sci. USA **85:**1749–1753.
12. **Horazdovsky, B., and R. Hogg.** 1989. Genetic reconstitution of high-affinity L-arabinose operon in *Escherichia coli*. J. Bacteriol. **171:**3053–3059.
13. **Hove-Jensen, B.** 1985. Cloning and characterization of the *prs* gene encoding phosphoribosyl pyrophosphate synthetase of *Escherichia coli*. Mol. Gen. Genet. **201:**269–276.
14. **Huo, L., K. Martin, and R. Schleif.** 1988. Alternative DNA loops regulate the arabinose operon in *Escherichia coli*. Proc. Natl. Acad. Sci. USA **85:**5444–5448.
15. **Johnson, C. M., and R. F. Schleif.** 1995. In vivo induction kinetics of the arabinose promoters in *Escherichia coli*. J. Bacteriol. **177:**3438–3442.
16. **Jordan, S. R., and C. O. Pabo.** 1988. Structure of the lambda complex at 2.5 resolution: details of the repressor-operator interactions. Science **242:**893–899.
17. **Kraus, A., C. Hueck, D. Gartner, and W. Hillen.** 1994. Catabolite repression of the *Bacillus subtilis xyl* operon involves a *cis* element functional in the context of an unrelated sequence, and glucose exerts additional *xylR*-dependent repression. J. Bacteriol. **176:**1738–1745.
18. **Laemni, U. K.** 1970. Cleavage of structural proteins during the assembly of the head of bacteriophage T4. Nature (London) **227:**680–685.
19. **Lin, E. C. C.** 1987. Dissimilatory pathways for sugars, polyols, and carboxylates, p. 244–284. *In* F. C. Neidhardt, J. L. Ingraham, K. B. Low, B. Magasanik, M. Schaechter, and H. E. Umbarger (ed.), *Escherichia coli* and *Salmonella typhimurium*: cellular and molecular biology. American Society for Microbiology, Washington, D.C.
20. **Lobell, R., and R. Schleif.** 1990. DNA looping and unlooping by AraC protein. Science **250:**528–532.
21. **Lobell, R., and R. Schleif.** 1991. AraC-DNA looping: orientation and distance-dependent loop breaking by the cyclic AMP receptor protein. J. Mol. Biol. **218:**45–54.
22. **Lowry, O. H., N. J. Rosebrough, A. L. Farr, and R. J. Randall.** 1951. Protein measurement with the Folin phenol reagent. J. Biol. Chem. **193:**265–275.
23. **Lu, Y., C. Flaherty, and W. Hendrickson.** 1992. AraC protein contacts asymmetric sites in the *Escherichia coli araFGH* promoter. J. Biol. Chem. **267:**24848–24857.
24. **Maleszka, R., P. Y. Wang, and H. Schneider.** 1982. A ColEI hybrid plasmid containing *Escherichia coli* genes complementing D-xylose negative mutants of *Escherichia coli* and *Salmonella typhimurium*. Can. J. Biochem. **60:**144–151.
25. **Martin, K., and R. F. Schleif.** 1986. The DNA loop model for *ara* repression: AraC protein occupies the proposed loop sites *in vivo* and repression-negative mutations lie in the same sites. Proc. Natl. Acad. Sci. USA **83:**3654–3658.
26. **Maxam, A., and W. Gilbert.** 1977. A new method for sequencing DNA. Proc. Natl. Acad. Sci. USA **74:**560–564.
27. **Miller, J. H.** 1972. Experiments in molecular genetics. Cold Spring Harbor Laboratory, Cold Spring Harbor, N.Y.
28. **Novotny, C., and E. Englesberg.** 1966. The L-arabinose permease system in *Escherichia coli* B/r. Biochim. Biophys. Acta **117:**217–230.
29. **Ogden, S., D. Haggerty, C. M. Stoner, D. Kolodrubetz, and R. Schleif.** 1980. The *Escherichia coli* L-arabinose operon: binding sites of the regulatory protein and a mechanism of positive and negative regulation. Proc. Natl. Acad. Sci. USA **77:**3346–3350.
30. **Park, C., and G. L. Hazelbauer.** 1986. Mutations specifically affecting ligand interaction of Trg chemosensory transducer. J. Bacteriol. **167:**101–109.
31. **Powell, B. S., D. L. Court, Y. Nakamura, M. P. Rivas, and C. L. Turnbough.** 1994. Rapid confirmation of single copy lambda prophage integration by PCR. Nucleic Acids Res. **22:**5765–5766.
32. **Reeder, T., and R. Schleif.** 1991. Mapping, sequence, and apparent lack of function of *araJ*, a gene of the *Escherichia coli* arabinose regulon. J. Bacteriol. **173:**7765–7771.
33. **Reeder, T., and R. Schleif.** 1993. AraC protein can activate transcription from only one position and when pointed in only one direction. J. Mol. Biol. **231:**205–218.
34. **Rosenfeld, S. A., P. E. Steve, and N. W. Y. Ho.** 1984. Cloning and characterization of the *xyl* genes from *Escherichia coli*. Mol. Gen. Genet. **194:**410–415.
35. **Rygus, T., and W. Hillen.** 1992. Catabolite repression of the *xyl* operon in *Bacillus megaterium*. J. Bacteriol. **174:**3049–3055.
36. **Sambrook, J., E. F. Fritsch, and T. Maniatis.** 1989. Molecular cloning: a laboratory manual, 2nd ed. Cold Spring Harbor Laboratory, Cold Spring Harbor, N.Y.
37. **Scheler, A., and W. Hillen.** 1994. Regulation of xylose utilization in *Bacillus licheniformis*; Xyl-repressor-*xyl*-operator interaction studied by DNA modification protection and interference. Mol. Microbiol. **13:**505–512.
38. **Scripture, J. B., C. Voelker, S. Miller, R. T. O'Donnell, L. Polgar, J. Rade, B. F. Horazdovsky, and R. W. Hogg.** 1987. High-affinity L-arabinose transport operon. Nucleotide sequence and analysis of gene products. J. Mol. Biol. **197:**37–46.
39. **Shamanna, D. K., and K. E. Sanderson.** 1979. Uptake and catabolism of xylose in *Salmonella typhimurium* LT2. J. Bacteriol. **139:**64–70.
40. **Shamanna, D. K., and K. E. Sanderson.** 1979. Genetics and regulation of D-xylose utilization in *Salmonella typhimurium* LT2. J. Bacteriol. **139:**71–79.
41. **Simons, R. W., F. Houman, and N. Kleckner.** 1987. Improved single and multicopy lac-based vectors for protein and operon fusion. Gene **53:**85–96.
42. **Sizemore, C., B. Wieland, F. Gotz, and W. Hillen.** 1992. Regulation of *Staphylococcus xylosus* xylose utilization genes at the molecular level. J. Bacteriol. **174:**3042–3048.
43. **Sofia, H. J., V. Burland, D. L. Daniels, G. Plunkett III, and F. Blattner.** 1994. Analysis of the *Escherichia coli* genome. V. DNA sequence of the region from 76.0 to 81.5 minutes. Nucleic Acids Res. **22:**2576–2584.
44. **Song, S., and C. Park.** Unpublished data.
45. **Tobin, J. F., and R. F. Schleif.** 1990. Purification and properties of RhaR, the positive regulator of the L-rhamnose operons of *E. coli*. J. Mol. Biol. **211:**75–89.
46. **Tsung, K., R. E. Brissette, and M. Inouye.** 1989. Identification of the DNA-binding domain of the OmpR protein required for transcriptional activation of the *ompF* and *ompC* genes of *Escherichia coli* by *in vivo* DNA footprinting. J. Biol. Chem. **264:**10104–10109.
47. **Wilcox, G., et al.** 1974. Regulation of the L-arabinose operon *BAD in vitro*. J. Biol. Chem. **249:**2946–2952.
48. **Wilmes-Riesenberg, M. R., and B. L. Wanner.** 1992. Tn*phoA* and Tn*phoA′* elements for making and switching fusions for study of transcription, translation, and cell surface localization. J. Bacteriol. **174:**4558–4575.
49. **Wolberger, C., Y. Dong, M. Ptashne, and S. C. Harrison.** 1988. Structure of a phage 434 Cro/DNA complex. Nature (London) **335:**789–795.
50. **Xu, J., and R. C. Johnson.** 1995. Identification of genes negatively regulated by Fis: Fis and RpoS comodulate growth-phase-dependent gene expression in *Escherichia coli*. J. Bacteriol. **177:**938–947.
51. **Xu, J., and R. C. Johnson.** 1995. Fis activates the RpoS-dependent stationary-phase expression of *proP* in *Escherichia coli*. J. Bacteriol. **177:**5222–5231.